



Treatment of recalcitrant crystalline polysaccharides with lytic polysaccharide monooxygenase relieves the need for glycoside hydrolase processivity

Anne Grethe Hamre, Anne-Grethe Skaarberg Strømnes, Daniel Gustavsen, Gustav Vaaje-Kolstad, Vincent G.H. Eijsink, Morten Sørli^{*}

Department of Chemistry, Biotechnology and Food Science, Norwegian University of Life Sciences, PO 5003, N-1432, Ås, Norway

ARTICLE INFO

Keywords:

Processivity
Glycoside hydrolase
Lytic polysaccharide monooxygenase
Recalcitrant polysaccharides

ABSTRACT

Processive glycoside hydrolases associate with recalcitrant polysaccharides such as cellulose and chitin and repeatedly cleave glycosidic linkages without fully dissociating from the crystalline surface. The processive mechanism is efficient in the degradation of insoluble substrates, but comes at the cost of reduced enzyme speed. We show that less processive chitinase variants with reduced ability to degrade crystalline chitin, regain much of this ability when combined with a lytic polysaccharide monooxygenase (LPMO). When combined with an LPMO, several less processive chitinase mutants showed equal or even increased activity on chitin compared to the wild-type. Thus, LPMOs affect the need for processivity in polysaccharide degrading enzyme cocktails, which implies that the composition of such cocktails may need reconsideration.

1. Introduction

Chitin and cellulose represent some of nature's largest reservoirs of organic carbon in the form of monomeric hexose sugars (*N*-acetyl-glucosamine and glucose, respectively) linearly linked by β -1,4 glycosidic bonds. In their natural form, both polysaccharides are organized in crystalline arrangements that make up robust biological structures including crustacean cuticles (chitin) and plant cell walls (cellulose). Although these crystalline arrangements are crucial for biological function, they present a significant challenge in industrial utilization of biomass, where efficient enzymatic depolymerization is a critical step.

Enzymatic degradation of recalcitrant polysaccharides is thought to occur primarily through the synergistic action of glycoside hydrolases (GHs) that have complementary activities [1,2]. Endo-acting GHs make random scissions on the polysaccharide chains, whereas exo-acting GHs mainly target reducing and non-reducing chain ends. Both endo- and exo-acting GHs may be processive, which implies that they repeatedly cleave glycosidic linkages without fully dissociating from the crystalline surface. Lytic polysaccharide monooxygenases (LPMO) add to the degradation process by using a reduced oxygen species to cleave glycosidic bonds in crystalline regions, thus creating new chain ends for exo-acting GHs [3–6]. Processive GHs are typically the most abundant enzymes in both natural secretomes and industrial enzyme cocktails by

virtue of their significant hydrolytic potential on crystalline substrates [7]. LPMOs also make considerable contributions to the overall efficiency of cellulolytic enzyme cocktails [8], but the interplay between LPMOs and individual (processive) GHs is not well understood.

Processive GHs have active site tunnels or deep clefts aligned with surface exposed aromatic amino acids that provide strong binding to the substrate [9–14]. Aromate-mediated carbohydrate recognition facilitates the necessary fluid binding to the crystalline polymers, increases the efficiency of substrate degradation, and may provide a necessary pushing potential to overcome substrate obstacles that otherwise could have led to stalling of the enzyme [14–20]. The cost of the processive mechanism is loss of enzyme speed as the required strong interactions make the enzymes intrinsically slow. Indeed, studies of processive chitinases [16,20] have shown that replacement of aromatic amino acids by alanine led to reduced processivity and decreased activity on crystalline chitin, while yielding an up to 30-fold increase in the rate of hydrolysis of water soluble chitosan. A consequence is that, in some cases, it might be better to focus strategies for enzymatic depolymerization of polysaccharide biomass on improving substrate accessibility for non-processive enzymes rather than on improving the properties of processive enzymes [16]. Such strategies could include the use of LPMOs, which are known to disrupt the crystalline structure of chitin and cellulose [6,21–23].

^{*} Corresponding author.

E-mail address: morten.sorlie@nmbu.no (M. Sørli).

<https://doi.org/10.1016/j.carres.2019.01.001>

Received 24 August 2018; Received in revised form 5 December 2018; Accepted 5 January 2019

Available online 07 January 2019

0008-6215/ © 2019 The Authors. Published by Elsevier Ltd. This is an open access article under the CC BY-NC-ND license (<http://creativecommons.org/licenses/by-nc-nd/4.0/>).

In this work, we have investigated how treatment with a chitin-active LPMO affects the initial rate of chitin hydrolysis by engineered variants of two exo-processive chitinases from *Serratia marcescens* with different degrees of processivity. The results show that the LPMO makes the crystalline material more amenable to the action of chitinase variants with reduced processivity, and have potential implications for the future design of enzyme cocktails for conversion of recalcitrant polysaccharides.

2. Materials and methods

2.1. Chemicals

Chito-oligosaccharides (CHOS) were purchased from Megazyme (Wicklow, Ireland). Squid pen β -chitin was purchased from France Chitine (180 μ m microparticulate, Marseille, France). All other chemicals were of analytical grade and purchased from standard manufacturers.

2.2. Site-directed mutagenesis

Most chitinase variants used in this study have been described previously. Variants *SmChiB-F190A* and *SmChiB-F190A/W220A* (using *SmChiB-WT* and *SmChiB-F190A* as template, respectively) were generated using the QuikChange site directed mutagenesis kit from Stratagene (La Jolla, CA, USA), mainly as described by the manufacturer. The primers used for the mutagenesis are listed in Table 1 and were purchased from Life Technologies (Carlsbad, CA, USA). To confirm that the gene contained the desired mutation and to check for the occurrence of non-desirable mutations, the mutated genes were sequenced using the LIGHTrun sequencing service of GATC Biotech (Constance, Germany), before they were transformed into *Escherichia coli* BL21Star (DE3) cells (Life Technologies).

2.3. Protein expression and purification

The chitinases were from *S. marcescens* strain BJL200 [24,25]. *SmChiA-WT*, *SmChiB-WT*, *SmChiA-W167A*, *SmChiA-W275A*, *SmChiB-W97A*, *SmChiB-W220A*, *SmChiB-W97A/W220A*, and *SmChiB-F190A* were expressed in *E. coli* as described previously [16,20,26]. The same applies for *SmLPMO10A* (previously known as CBP21) [27]. The periplasmic extracts were loaded on a column packed with chitin beads (New England Biolabs, Ipswich, MA, USA) equilibrated in 50 mM Tris-HCl pH 8.0 (chitinases) or 50 mM Tris-HCl pH 8.0, 1 M ammonium sulfate (*SmLPMO10A*). After washing the column with the same buffer, the enzymes were eluted with 20 mM acetic acid. Purified proteins were further concentrated by use of Macrosep® Advances Centrifugal Devices (PALL Corporation, New York, NY) with a molecular mass cutoff of 30000 Da (chitinases) or Amicon Ultra Centrifugal filters (Merck Millipore, Darmstadt, Germany) with a molecular mass cutoff of 10000 Da (*SmLPMO10A*). The chitinases and *SmLPMO10A* were stored at 4 °C in 100 mM Tris-HCl pH 8.0 or 50 mM sodium acetate buffer pH 6.1, respectively.

The *SmChiB-F190A/W220A* gene was expressed as described previously for wild type *SmChiB* and its mutants [16,24]. The periplasmic extract was adjusted to Buffer A (50 mM Tris-HCl pH 8.0, 1 M

(NH₄)₂SO₄) with 3 M (NH₄)₂SO₄ and loaded onto a HiTrap Phenyl HP column (5 mL) (GE Healthcare, Little Chalfont, Great Britain) connected to a BioLogic low-pressure protein purification system (Bio-Rad, Hercules, CA, USA). The chitinase was eluted by applying a two-step gradient where the first step was a linear salt gradient from 100% buffer A to 70% buffer B (50 mM Tris-HCl pH 8.0) over 10 column volumes at a flow rate of 4 mL/min. The second step was a new linear salt gradient from 70 to 100% buffer B over 15 column volumes at a flow rate of 4 mL/min. Finally, buffer B was applied for 5 column volumes. The chitinase containing fractions were detected by SDS-PAGE, pooled and concentrated to 1 mL, using Macrosep® Advances Centrifugal Devices (PALL Corporation) with a molecular mass cutoff of 30000 Da. Subsequently, samples were loaded onto a HiLoad 16/600 Superdex 75 Prepgrade column (GE Healthcare), with a running buffer consisting of 20 mM Tris-HCl pH 8.0 and 0.2 M NaCl, using a flow rate of 1 mL/min. The chitinase eluted approximately 60 min after injection. The buffer was changed to 100 mM Tris-HCl pH 8.0 using Macrosep® Advances Centrifugal Devices (30000 Da cutoff) (PALL Corporation).

For all enzymes, chitinases and *SmLPMO10A*, enzyme purity was verified by SDS-PAGE and the enzyme concentration was estimated by using the Bradford Protein Assay from Bio-Rad.

2.4. Time course of chitin degradation

Hydrolysis of chitin (20 mg/mL) was carried out in 50 mM sodium acetate at pH 6.1. Previously, we have shown that 20 mg/mL chitin gives substrate saturating conditions [3]. The chitin samples were sonicated for 20 min in a sonication bath (Transonic Elma) to increase the surface of the substrate and thereby increase the availability of chitin ends for the enzymes [28]. The reaction tubes were incubated at 37 °C in an Eppendorf thermomixer at 800 rpm. The chitinase concentration was 100 nM in all experiments. Aliquots of 75 μ L were withdrawn every hour for 7 h, and the enzymes were inactivated by adding 75 μ L 20 mM H₂SO₄. Prior to further HPLC analysis all samples were filtrated through a 0.45 μ m Duapore membrane (Merck Millipore) to remove denatured protein and chitin particles. All reactions were run in, at least, triplicate, and all samples were stored at –20 °C until HPLC analysis.

2.5. Time course of chitin degradation after treatment with *SmLPMO10A*

The degradation was carried out as described in section 2.4 with the following exception: After sonication, *SmLPMO10A* and ascorbic acid were added to an end concentration of 1 μ M and 2 mM, respectively. The samples were incubated at 37 °C in an Eppendorf thermomixer at 800 rpm for 2.5 h before the addition of chitinase.

2.6. Determination of apparent degree of processivity

In this work, apparent degree of processivity was assessed on the basis of the initial [(GlcNAc)₂]/[GlcNAc] product ratio from chitin hydrolysis as described in Hamre et al. [15]. Hydrolysis of chitin (2.0 mg/mL) was carried out in 50 mM sodium acetate buffer at pH 6.1. The chitin samples were sonicated for 20 min in a sonication bath (Transonic, Elma). The reaction tubes were then incubated at 37 °C in an Eppendorf thermomixer at 800 rpm to avoid settling of the chitin particles. The chitinase concentration was 2.5 μ M. Aliquots of 75 μ L were withdrawn at regular time intervals, and the enzymes were inactivated by adding 75 μ L 20 mM H₂SO₄. Prior to further HPLC analysis all samples were filtrated through a 0.45 μ m Duapore membrane (Merck Millipore) to remove denatured protein and chitin particles. All reactions were performed in duplicate, and all samples were stored at –20 °C until HPLC analysis.

Table 1
Primes used for site-directed mutagenesis.

Enzyme	Primer	Sequence
ChiB-F190A	forward	5'-GCCGGCGGGCGCCCTTCTGTGCGG-3'
	reverse	5'-CGCGACAGGAAGCGGCGCCGCGGC-3'
ChiB-F190A/W220A	forward	5'-TGGCGGCGCCCGCGGAGAAG-3'
	reverse	5'-CTTCTCCGGGGCGCGGCA-3'

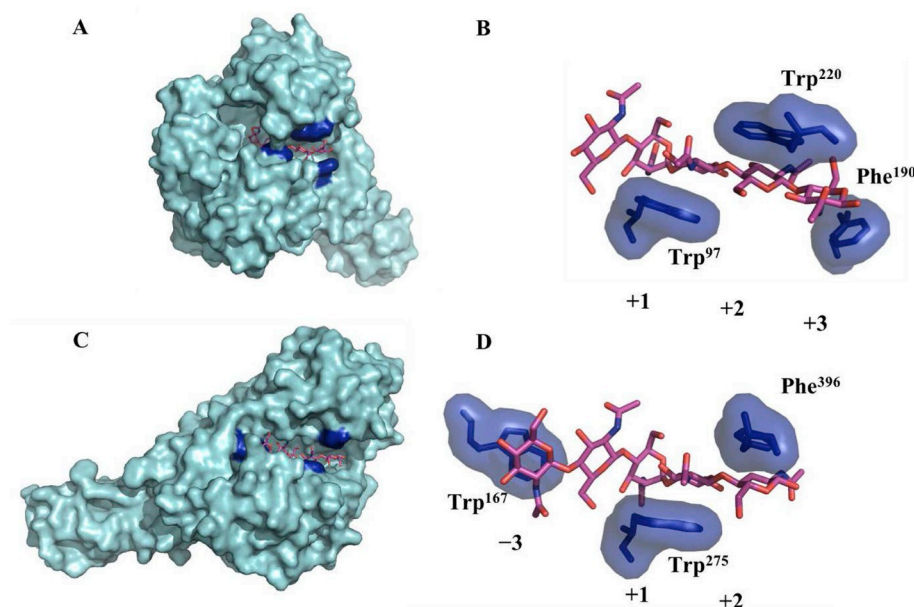


Fig. 1. Substrate binding in *SmChiA* and *SmChiB*. The panels show structurally aligned crystal structures of *SmChiB* (A&B; pdb 1e6n [31]) and *SmChiA* (C&D; pdb 1ehn [32]) with substrates. Selected surface exposed aromatic amino acids are highlighted in blue. (For interpretation of the references to colour in this figure legend, the reader is referred to the Web version of this article.)

2.7. High performance liquid chromatography (HPLC)

Concentrations of mono- and disaccharides were determined using a Dionex Ultimate 3000 UHPLC system (Dionex Corp., Sunnyvale, CA, USA) equipped with a Rezex Fast fruit H⁺ column (100 mm length and 7.8 mm inner diameter) (Phenomenex, Torrance, CA, USA). The sample size was 8 μ L, and the mono- and disaccharides were eluted isocratically at 1 mL/min with 5 mM H₂SO₄ at 85 °C. The mono- and disaccharides were monitored by measuring absorbance at 195 nm, and the amounts were quantified by measuring peak areas. Peak areas were compared with peak areas obtained with standard samples with known concentrations of mono- and disaccharides. The degree of degradation (in percent) is defined as the amount of solubilized GlcNAc units divided by the amount of GlcNAc units in the chitin polymer at the start of the experiment.

2.8. Determination of A- and b-values for activity

According to Kostylev and Wilson, the following two-parameter kinetic model can be used to determine a time-dependent activity constant for polysaccharide degradation by a glycoside hydrolase:

$$X = At^b \quad (1)$$

where t is time (h), X is degree of degradation (in percent) is defined as the amount of solubilized GlcNAc units divided by the amount of GlcNAc units in the chitin polymer at the start of the experiment, A is the activity of the added enzyme, and b is an intrinsic constant that quantifies the curvature of the time course profile [29]. A and b values were determined after fitting the data from chitin degradation reactions to equation (1) by use of Origin Pro 7.5 Software.

3. Results and discussion

Serratia marcescens is a soil bacterium that produces four chitin-depolymerizing enzymes: *SmChiC*, an endo-nonprocessive chitinase, *SmChiA* and *SmChiB*, two exo-processive chitinases moving along chitin chains in opposite directions, and *SmLPMO10A*, a surface-active lytic polysaccharide monooxygenase, also known as CBP21, that introduces chain breaks by oxidative cleavage [30]. Previous studies have shown that aromatic amino acids in so-called substrate binding subsites, i.e. subsites interacting with the polymeric part of the chitin chain during processive action, are crucial for the processive ability of *SmChiA* and

SmChiB [16,20].

In *SmChiB*, residues important for processivity include Trp⁹⁷ (subsite +1), Trp²²⁰ (subsite +2), and Phe¹⁹⁰ (subsite +3) (Fig. 1). In *SmChiA*, Trp¹⁶⁷ in the substrate-binding subsite -3 is crucial for processivity, while processivity is also affected, albeit to a lesser extent by Trp²⁷⁵ and Phe³⁹⁶ in product binding subsites +1 and +2, respectively, where dimeric products are released during processive hydrolysis [20]. Processivity implies that upon hydrolysis and release of the dimeric product the enzyme has a larger change of rebinding compared to diffusing away from the remaining substrate and the impact of the product binding subsites in *SmChiA* is likely due to promoting rebinding [18,20].

Experimental assessment of processivity may be done using several methods but is not straightforward (see Horn et al. for further discussion [33]). The apparent processive ability (P^{app}) provides a quantitative parameter and is defined as the average number of catalytic acts that an enzyme performs per one initiation of a processive run, which may be derived from various types of experiments, each with potential limitations. In Fig. 2, we have illustrated how P^{app} can be determined from determination of the ratio of dimeric products vs. monomeric products, which is a “classical” method for processive GH action and used to for *SmChiB*-F190A in this study [33]. Regardless of these limitations, especially when it comes to quantification, available previous and newly generated data (Table 2) clearly show that all single mutants used in this study exhibit reduced processivity compared to the wild types.

Assessing kinetics of GH catalyzed hydrolysis of recalcitrant polysaccharides are not trivial [34]. It is very common to observe nonlinear behavior at a low degree of substrate conversion [19,29]. Different enzyme- and substrate-related factors can be responsible for the rapid decrease in hydrolysis rates such as the substrate being heterogeneous resulting in different parts being degraded faster than others, and that GHs tend to get stuck on the surface [17,34,35]. Kostylev and Wilson have developed a simple two-parameter equation (Equation (1)) to tackle this. One of the parameters is a total activity coefficient and the other is an intrinsic constant that reflects the ability of the GHs to overcome the varying degree of substrate recalcitrance. This properly addresses the observed nonlinearities and allows for the direct comparison between different GH actions on the same substrate [29]. Since all wild types and mutated variants showed nonlinear rates in the presences of *SmLPMO10A*, we opted to use Equation (1) in our kinetic analysis. It is proposed that LPMO action create new chain ends, and by

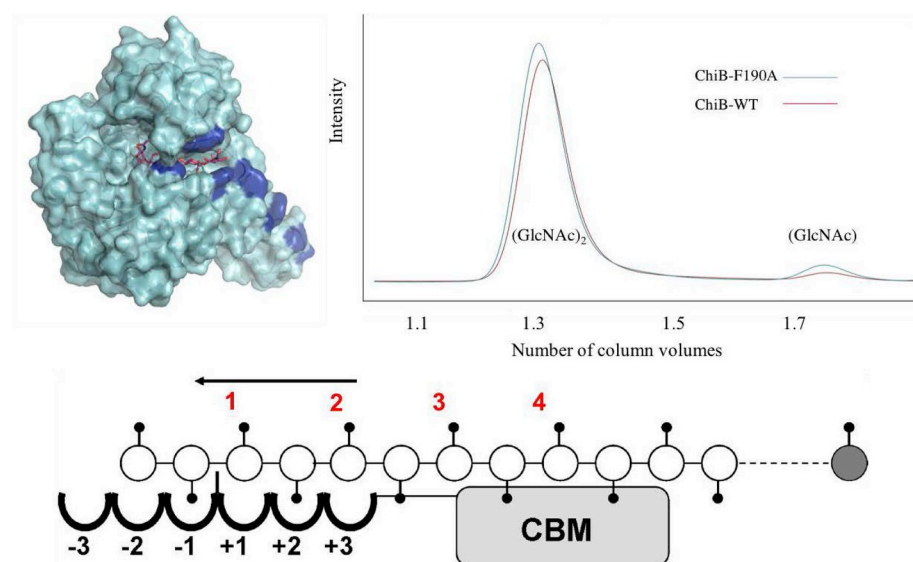


Fig. 2. Crystal structure of *SmChiB* (top left) and a schematic picture of *SmChiB* in complex with a single chitin chain (bottom). Surface exposed aromatic amino acids stacking with sugar moieties (being individual subsites) are highlighted in blue. The glycosidic bond between the sugar residues in subsite -1 and $+1$ is enzymatically cleaved. A correctly positioned *N*-acetyl group (shown as sticks) in the -1 subsite is essential for the substrate-assisted catalysis. Due to that the smallest structural unit of chitin is a disaccharide, the product of repeated processive enzymatic actions will be dimers, (GlcNAc)₂. Monomers, GlcNAc, originate from initial productive binding when the sugar in the non-reducing end occupies a subsite with an odd number. Hence, a high ratio of [(GlcNAc)₂]/[GlcNAc] indicates a high degree of apparent processivity. A chromatogram (top right) of (GlcNAc)₂ and GlcNAc resulting from chitin degradation (4%) is shown for *SmChiB*-F190A (red line) and compared to that of *SmChiB*-WT (blue line). *SmChiA*-F190A is less processive ($P^{app} = 11.6$) than *SmChiB*-WT ($P^{app} = 24.3$) thus producing higher concentrations of GlcNAc than the wild type. (For interpretation of the references to colour in this figure legend, the reader is referred to the Web version of this article.)

this will increase the heterogeneity of the substrate. All *SmChiB* mutated variants showed activities (A values) amounting to approximately 15% of the wild type activity (Table 2 and Fig. 3). As expected, the addition of *SmLPMO10A* resulted in an increase (13-fold) in *SmChiB* activity. Remarkably, the effect of *SmLPMO10A* on less processive *SmChiB* variants was much more pronounced. For example, the activity of *SmChiB*-W97A was increased 55-fold and in the presence of *SmLPMO10A* the activity was 65% of the wild type, as opposed to 16% in the absence of *SmLPMO10A*. Likewise, addition of *SmLPMO10A* yielded a 68-fold increase in the activity of *SmChiB*-F190A and the activity was equal to that of the wild type enzyme. Interestingly, chitin hydrolysis by *SmChiB*-W220A became 160-fold faster in the presence of *SmLPMO10A* making this mutant 1.55-fold more active than the wild type enzyme. In the presence of *SmLPMO10A*, each of the double mutants displayed activities similar to the wild type enzyme.

Interestingly, the presence of *SmLPMO10A* resulted in less activation of *SmChiA* compared to *ChiB* (7-fold vs. 13-fold), in line with previous results [3]. Also for *SmChiA*, the presence of *SmLPMO10A* caused rate enhancements for the less processive mutants that were larger compared to the wild-type, but to a lesser degree than for the *SmChiB* mutants (30- and 12-fold increase for *SmChiA*-W167A and *SmChiA*-275A, respectively). Furthermore, in the presence of *SmLPMO10A* the activities of the less processive mutants only reached 66% and 48%, respectively, of the wild type activity (as compared to up to 155% for *SmChiB*-W220A).

From these results, it is clear that the need for processivity in enzymatic degradation of polysaccharides may be reduced when the crystalline substrate is treated with an LPMO. The trends are the same for all less processive variants, but the clearest example is provided by *SmChiB*-W220A, which in reactions with *SmLPMO10A* displayed a 55% increase in activity compared to the wild type under identical conditions. Crystallographic studies (Fig. 1) show that Trp²²⁰ interacts closely with the substrate, thus likely making a major contribution to keeping the enzyme closely associated to the substrate in between subsequent hydrolytic reactions and preventing once-detached single chains from re-associating with the insoluble material [16,36]. Having access to numerous new chain ends provided by the LPMO likely reduces the beneficial effect of the “stickiness” provided by Trp²²⁰ (and other aromatic residues near the catalytic center). This reasoning is in line with the notion that the rate-determining step for chitinase catalyzed hydrolysis changes from substrate association, for chitin, to

Table 2

Activity on β -chitin in the absence and presence of *SmLPMO10A* for *SmChiA* and *SmChiB* and mutants investigated in this study.

Enzyme	A	b	P^{app} , ^a	P^{app} , ^b
<i>SmChiA</i>				
WT	0.32 ± 0.06	0.65 ± 0.13	30.1 ^c	36 ^d
W167A ^{*e}	0.05 ± 0.02	0.90 ± 0.25	n.a. ^f	16 ^d
W275A [*]	0.06 ± 0.02	0.62 ± 0.21	n.a. ^f	14 ^d
<i>SmChiA</i> with <i>SmLPMO10A</i>				
WT	2.29 ± 0.28	0.51 ± 0.08		
W167A	1.51 ± 0.08	0.38 ± 0.04		
W275A	1.09 ± 0.14	0.75 ± 0.07		
<i>SmChiB</i>				
WT	0.31 ± 0.04	0.73 ± 0.1	24.3 ^c	n.d. ^g
W97A [*]	0.05 ± 0.01	0.96 ± 0.1	11.0 ^c	n.d. ^g
W220A [*]	0.04 ± 0.01	1.16 ± 0.2	9.8 ^h	n.d. ^g
W97A/W220A	0.06 ± 0.01	0.54 ± 0.1	n.d. ^g	n.d. ^g
F190A	0.06 ± 0.01	0.84 ± 0.1	11.6 ^h	n.d. ^g
F190A/W220A	0.04 ± 0.01	0.78 ± 0.1	n.d. ^g	n.d. ^g
<i>SmChiB</i> with <i>SmLPMO10A</i>				
WT	4.16 ± 0.31	0.45 ± 0.05		
W97A	2.71 ± 0.23	0.40 ± 0.06		
W220A	6.48 ± 0.74	0.30 ± 0.08		
W97A/W220A	4.43 ± 0.33	0.23 ± 0.10		
F190A	4.06 ± 0.60	0.54 ± 0.09		
F190A/W220A	4.46 ± 0.20	0.37 ± 0.03		

^a As determined on the basis of the [(GlcNAc)₂]/[GlcNAc] product ratio during the initial phase of degradation of β -chitin [15].

^b As determined from the plot of the concentration of enzyme-generated reducing groups versus insoluble reducing groups upon chitin degradation under single-hit conditions [18].

^c Values obtained from Hamre et al. [15].

^d Values obtained from Kurašin et al. [18].

^e For mutants marked with a *, the loss of processivity has also been shown in experiments with chitosan; Se Horn et al. and Zakariassen et al. for more details [16,20].

^f Not applicable. An assumption for the use of the [(GlcNAc)₂]/[GlcNAc] product ratio upon degradation of β -chitin is that there should not be a significant different probability of endo-mode initiation between enzymes nor too high degree of endo-mode initiation. Since *ChiA*-W167A and *ChiB*-W275A display a high degree of endo-mode initiation that differs significantly from the wild type [18], this method is not used to assess P^{app} .

^g Not determined.

^h Determined in this work.

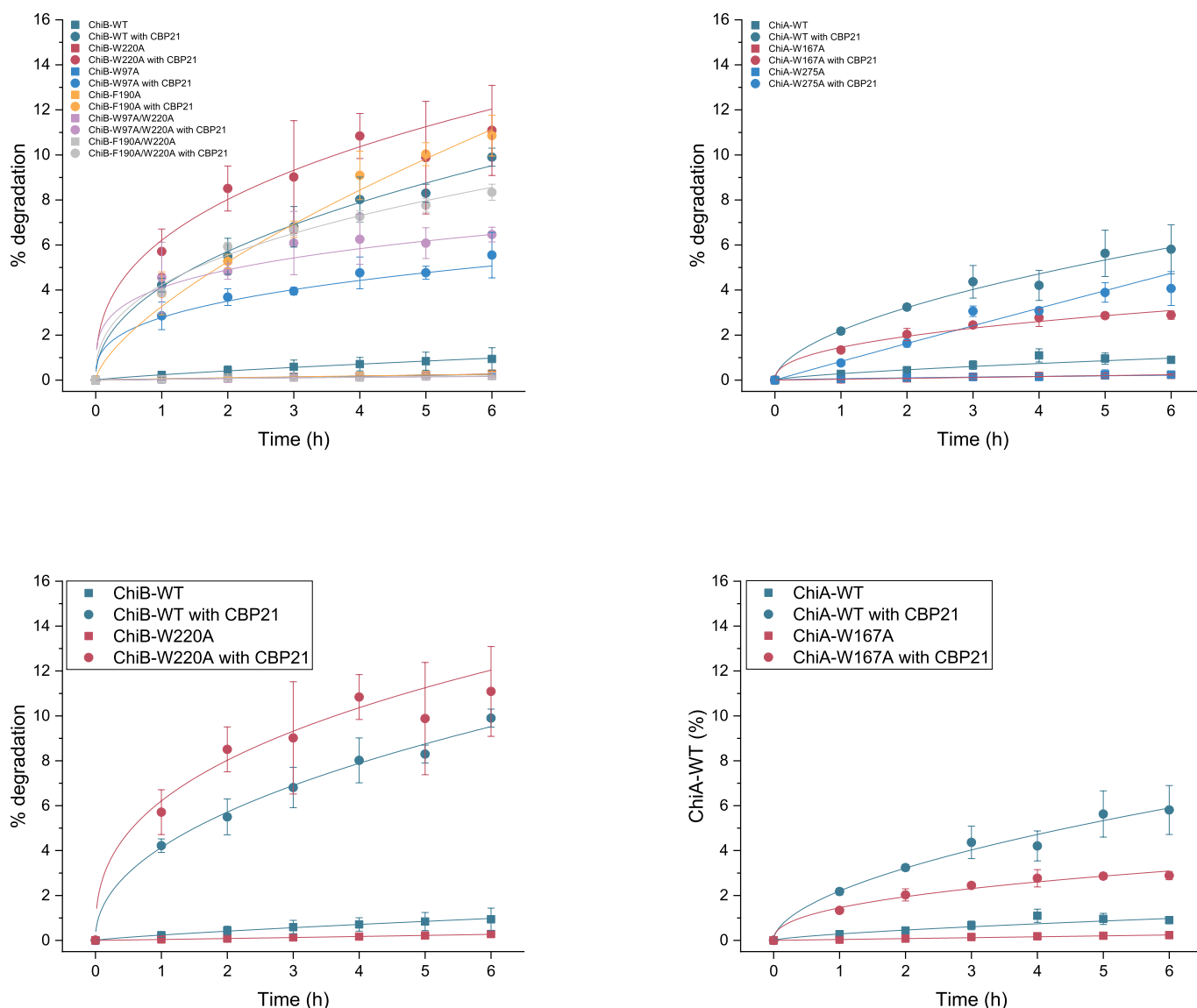


Fig. 3. Examples of progress curves fitted to Eq. (1). The top left panel shows data for *SmChiB*-WT (green), *SmChiB*-W220A (red), *SmChiB*-W97A (blue), *SmChiB*-F190A (orange), *SmChiB*-W97A/W220A (violet), and *SmChiB*-F190A/W220A (grey), with (circle) and without (square) *SmLPMO10A*. The top right panel shows data for *SmChiA*-WT (green), *SmChiA*-W167A (red), and *SmChiA*-W275A (blue), with (circle) and without (square) *SmLPMO10A*. The hydrolysis were performed with 100 nM enzyme in 50 mM sodium acetate pH 6.1 at 37 °C with 20 mg/ml chitin. The bottom left and right panels focus on the wild types of *SmChiB* and *SmChiA*, respectively, and the most active mutants, *SmChiB*-W220A and *SmChiA*-W167A. (For interpretation of the references to colour in this figure legend, the reader is referred to the Web version of this article.)

product displacement when the substrate becomes more available as in the soluble chitin variant chitosan [37].

It has been shown that Trp⁹⁷ (subsite +1) and Phe¹⁹⁰ (subsite +3) provide less binding free energy compared to Trp²²⁰ [11,38]. Moreover, While Trp²²⁰ seems only involved in substrate-binding and seems pre-ordered to do so in the apo-enzyme, Trp⁹⁷ has an additional catalytic role since it takes part in stabilizing the energetically demanding ⁴C₁ to ^{1,4}B conformational change of the *N*-acetylglucosamine in the −1 subsite [31,39]. Phe¹⁹⁰ shows a −91° rotation around χ_1 upon substrate binding [31], which may slightly offset the beneficial effect of the Phe-substrate interaction. These differences may underlie the observed variations in the rate enhancements observed upon adding *SmLPMO10A*.

Previous studies have shown that the initial rate of endo-non-processive *SmChiC* of *S. marcescens* is not enhanced by treatment with an LPMO, in line with the proposed main role of LPMOs to create new chain-ends for exo-acting GHs [3]. To this regard, it is interesting to

observe that the rate of hydrolysis is more enhanced for *SmChiB* than for *SmChiA*. It has been suggested that, when acting on chitin, *SmChiA* is the most endo-active of the two GHs [26]. Moreover, the mutation of either Trp¹⁶⁷ or Trp²⁷⁵ to Ala, changes the probability of endo mode-initiation of hydrolysis by *SmChiA* from 76% to 90% [18]. The increase in endo mode-initiation is one possible cause of the observed lower effect of *SmLPMO10A* on the efficiency of the *SmChiA* mutants compared to the *SmChiB* mutants.

The advent of LPMOs has already led to considerable improvements of enzyme cocktails for biomass processing [8,40], while recent results related to the nature of the co-substrate (O₂ or H₂O₂) and enzyme stability suggest that the potential of LPMOs has not yet been fully harnessed [41–43]. So far, the interplay between LPMOs and individual GHs with varying functionalities (endo-, exo-, processive) has not been studied in much detail. The present data show that the inclusion of LPMOs in enzyme cocktails may affect the need for certain GH types, in this case the highly “sticky” exoprocessive enzymes often referred to as

chito- or cello-biohydrolases. Thus, harnessing the full potential of LPMOs not only requires selection of the best LPMOs and LPMO-friendly processing conditions, but also a reconsideration of the glycoside hydrolase composition of polysaccharide degrading enzyme cocktails.

Acknowledgments

This work was supported by grants from the Norwegian Research Council 209335 (MS).

Appendix A. Supplementary data

Supplementary data to this article can be found online at <https://doi.org/10.1016/j.carres.2019.01.001>.

References

- [1] B. Henrissat, H. Driguez, C. Viet, M. Schulein, Synergism of cellulases from *Trichoderma reesei* in the degradation of cellulose, *Bio Technology* 3 (1985) 722–726.
- [2] S.T. Merino, J. Cherry, Progress and challenges in enzyme development for biomass utilization, *Adv. Biochem. Eng. Biotechnol.* 108 (2007) 95–120.
- [3] A.G. Hamre, K.B. Eide, H.H. Wold, M. Sørle, Activation of enzymatic chitin degradation by a lytic polysaccharide monooxygenase, *Carbohydr. Res.* 407 (2015) 166–169.
- [4] P.V. Harris, D. Welner, K.C. Mcfarland, E. Re, J.C. Navarro Poulsen, K. Brown, R. Salbo, H. Ding, E. Vlasenko, S. Merino, F. Xu, J. Cherry, S. Larsen, L. Lo Leggio, Stimulation of lignocellulosic biomass hydrolysis by proteins of glycoside hydrolase family 61: structure and function of a large, enigmatic family, *Biochemistry* 49 (2010) 3305–3316.
- [5] G. Vaaje-Kolstad, S.J. Horn, D.M. Van Aalten, B. Synstad, V.G.H. Eijsink, The non-catalytic chitin-binding protein CBP21 from *Serratia marcescens* is essential for chitin degradation, *J. Biol. Chem.* 280 (2005) 28492–28497.
- [6] G. Vaaje-Kolstad, B. Westereng, S.J. Horn, Z. Liu, H. Zhai, M. Sørle, V.G.H. Eijsink, An oxidative enzyme boosting the enzymatic conversion of recalcitrant polysaccharides, *Science* 330 (2010) 219–222.
- [7] G.T. Beckham, J. Ståhlberg, B.C. Knott, M.E. Himmel, M.F. Crowley, M. Sandgren, M. Sørle, C.M. Payne, Towards a molecular-level theory of carbohydrate processivity in glycoside hydrolases, *Curr. Opin. Struct. Biol.* 27 (2014) 96–106.
- [8] G. Müller, A. Várnai, K.S. Johansen, V.G.H. Eijsink, S.J. Horn, Harnessing the potential of LPMO-containing cellulase cocktails poses new demands on processing conditions, *Biotechnol. Biofuels* 8 (2015) 187.
- [9] F. Colussi, T.H. Sørensen, K. Alasepp, J. Kari, N. Cruys-Bagger, M.S. Windahl, J.P. Olsen, K. Borch, P. Westh, Probing substrate interactions in the active tunnel of a catalytically deficient cellobiohydrolase (Cel7), *J. Biol. Chem.* 290 (2015) 2444–2454.
- [10] G.J. Davies, B. Henrissat, Structures and mechanisms of glycosyl hydrolases, *Structure* 3 (1995) 853–859.
- [11] A.G. Hamre, E.E. Frøberg, V.G.H. Eijsink, M. Sørle, Thermodynamics of tunnel formation upon substrate binding in a processive glycoside hydrolase, *Arch. Biochem. Biophys.* 520 (2017) 35–42.
- [12] A.G. Hamre, S. Jana, M.M. Holen, G. Mathiesen, V. P, C.M. Payne, M. Sørle, Thermodynamic relationships with processivity in *Serratia marcescens* family 18 chitinases, *J. Phys. Chem. B* 119 (2015) 9601–9613.
- [13] J. Rouvinen, T. Bergfors, T. Teeri, J.K. Knowles, T.A. Jones, Three-dimensional structure of cellobiohydrolase II from *Trichoderma reesei*, *Science* 249 (1990) 380–386.
- [14] A. Varrot, T.P. Frandsen, I. Von Ossowski, V. Boyer, S. Cottaz, H. Driguez, M. Schulein, G.J. Davies, Structural basis for ligand binding and processivity in cellobiohydrolase Cel6A from *Humicola insolens*, *Structure* 11 (2003) 855–864.
- [15] A.G. Hamre, S.B. Lorentzen, P. Våljamäe, M. Sørle, Enzyme processivity changes with the extent of recalcitrant polysaccharide degradation, *FEBS Lett.* 588 (2014) 4620–4624.
- [16] S.J. Horn, P. Sikorski, J.B. Cederkvist, G. Vaaje-Kolstad, M. Sørle, B. Synstad, G. Vriend, K.M. Vårum, V.G.H. Eijsink, Costs and benefits of processivity in enzymatic degradation of recalcitrant polysaccharides, *Proc. Natl. Acad. Sci. U.S.A.* 103 (2006) 18089–18094.
- [17] K. Igarashi, T. Uchihashi, A. Koivula, M. Wada, S. Kimura, T. Okamoto, M. Penttilä, T. Ando, M. Samejima, Traffic jams reduce hydrolytic efficiency of cellulase on cellulose surface, *Science* 333 (2011) 1279–1282.
- [18] M. Kurašin, S. Kuusk, P. Kuusk, M. Sørle, P. Våljamäe, Slow off-rates and strong product binding are required for processivity and efficient degradation of recalcitrant chitin by family 18 chitinases, *J. Biol. Chem.* 290 (2015) 29074–29085.
- [19] S. Kuusk, M. Sørle, P. Våljamäe, The predominant molecular state of bound enzyme determines the strength and type of product inhibition in the hydrolysis of recalcitrant polysaccharides by processive enzymes, *J. Biol. Chem.* 290 (2015) 11678–11691.
- [20] H. Zakariassen, B.B. Aam, S.J. Horn, K.M. Vårum, M. Sørle, V.G.H. Eijsink, Aromatic residues in the catalytic center of chitinase A from *Serratia marcescens* affect processivity, enzyme activity, and biomass converting efficiency, *J. Biol. Chem.* 284 (2009) 10610–10617.
- [21] M. Eibinger, T. Ganner, P. Bubner, S. Rošker, D. Kracher, D. Haltrich, R. Ludwig, H. Plank, B. Nidetzky, Cellulose surface degradation by a lytic polysaccharide monooxygenase and its effect on cellulase hydrolytic efficiency, *J. Biol. Chem.* 289 (2014) 35929–35938.
- [22] B. Song, B. Li, X. Wang, W. Shen, S. Park, C. Collings, A. Feng, S.J. Smith, J.D. Walton, S.-Y. Ding, Real-time imaging reveals that lytic polysaccharide monooxygenase promotes cellulase activity by increasing cellulose accessibility, *Biotechnol. Biofuels* 11 (2018) 41.
- [23] A. Villares, C. Moreau, C. Bennati-Granier, S. Garajova, L. Foucat, X. Falourd, B. Saake, J.-G. Berrin, B. Cathala, Lytic polysaccharide monooxygenases disrupt the cellulose fibers structure, *Sci. Rep.* 7 (2017) 40262.
- [24] M.B. Brurberg, V.G. Eijsink, A.J. Haandrikman, G. Venema, I.F. Nes, Chitinase B from *Serratia marcescens* BJL200 is exported to the periplasm without processing, *Microbiology* 141 (Pt 1) (1995) 123–131.
- [25] M.B. Brurberg, V.G. Eijsink, I.F. Nes, Characterization of a chitinase gene (chiA) from *Serratia marcescens* BJL200 and one-step purification of the gene product, *FEMS Microbiol. Lett.* 124 (1994) 399–404.
- [26] M.B. Brurberg, I.F. Nes, V.G.H. Eijsink, Comparative studies of chitinases A and B from *Serratia marcescens*, *Microbiology* 142 (1996) 1581–1589.
- [27] G. Vaaje-Kolstad, D.R. Houston, A.H. Riemen, V.G. Eijsink, D.M. Van Aalten, Crystal structure and binding properties of the *Serratia marcescens* chitin-binding protein CBP21, *J. Biol. Chem.* 280 (2005) 11313–11319.
- [28] Y. Fan, T. Saito, A. Isogai, Preparation of chitin nanofibers from squid pen β -chitin by simple mechanical treatment under acid conditions, *Biomacromolecules* 9 (2008) 1919–1923.
- [29] M. Kostylev, D. Wilson, Two-parameter kinetic model based on a time-dependent activity coefficient accurately describes enzymatic cellulose digestion, *Biochemistry* 52 (2013) 5656–5664.
- [30] G. Vaaje-Kolstad, S.J. Horn, M. Sørle, V.G.H. Eijsink, The chitinolytic machinery of *Serratia marcescens* – a model system for enzymatic degradation of recalcitrant polysaccharides, *FEBS J.* 280 (2013) 3028–3049.
- [31] D.M.F. van Aalten, D. Komander, B. Synstad, S. Gåseidnes, M.G. Peter, V.G.H. Eijsink, Structural insights into the catalytic mechanism of a family 18 exochitinase, *Proc. Natl. Acad. Sci. U. S. A.* 98 (2001) 8979–8984.
- [32] Y. Papanikolaou, G. Prag, G. Tavlas, C.E. Vorgias, A.B. Oppenheim, K. Petratos, High resolution structural analyses of mutant chitinase A complexes with substrates provide new insight into the mechanism of catalysis, *Biochemistry* 40 (2001) 11338–11343.
- [33] S.J. Horn, M. Sørle, K.M. Vårum, P. Våljamäe, V.G.H. Eijsink, Measuring Processivity, *Meth. Enzymol.*, Academic Press, 2012.
- [34] P. Bansal, M. Hall, M.J. Reaff, J.H. Lee, A.S. Bommaris, Modeling cellulase kinetics on lignocellulosic substrates, *Biotechnol. Adv.* 27 (2009) 833–848.
- [35] M. Kurašin, P. Våljamäe, Processivity of cellobiohydrolases is limited by the substrate, *J. Biol. Chem.* 286 (2011) 169–177.
- [36] T.T. Teeri, Crystalline cellulose degradation: new insight into the function of cellobiohydrolases, *Trends Biotechnol.* 15 (1997) 160–167.
- [37] H. Zakariassen, V.G.H. Eijsink, M. Sørle, Signatures of activation parameters reveal substrate-dependent rate determining steps in polysaccharide turnover by a family 18 chitinase, *Carbohydr. Polym.* 81 (2010) 14–20.
- [38] S. Jana, A.G. Hamre, P. Wildberger, M.M. Holen, V.G.H. Eijsink, G.T. Beckham, M. Sørle, C.M. Payne, Aromatic-mediated carbohydrate recognition in processive *Serratia marcescens* chitinases, *J. Phys. Chem. B* 120 (2016) 1236–1249.
- [39] X. Biarnes, A. Ardevol, A. Planas, C. Rovira, A. Laio, M. Parrinello, The conformational free energy landscape of f-d-glucopyranose. Implications for substrate preactivation in f-glucoside hydrolases, *J. Am. Chem. Soc.* 129 (2007) 10686–10693.
- [40] K.S. Johansen, Discovery and industrial applications of lytic polysaccharide monooxygenases, *Biochem. Soc. Trans.* 44 (2016) 143–149.
- [41] B. Bissaro, A.K. Röhr, M. Skaugen, Z. Forsberg, S.J. Horn, G. Vaaje-Kolstad, V.G.H. Eijsink, Oxidative cleavage of polysaccharides by monooxygenases depends on H₂O₂, *Nat. Chem. Biol.* 13 (2017) 1123–1128.
- [42] S. Kuusk, B. Bissaro, P. Kuusk, Z. Forsberg, V.G.H. Eijsink, M. Sørle, P. Våljamäe, Kinetics of H₂O₂-driven degradation of chitin by a bacterial lytic polysaccharide monooxygenase, *J. Biol. Chem.* 293 (2018) 523–531.
- [43] G. Müller, P. Chylenski, B. Bissaro, V.G.H. Eijsink, S.J. Horn, The impact of hydrogen peroxide supply on LPMO activity and overall saccharification efficiency of a commercial cellulase cocktail, *Biotechnol. Biofuels* 11 (2018) 209.